


## Article

# Modification of Taxifolin Properties by Spray Drying

Amir Taldaev <sup>1,2</sup>, Roman P. Terekhov <sup>2,\*</sup> , Irina A. Selivanova <sup>2</sup>, Denis I. Pankov <sup>2</sup>, Maria N. Anurova <sup>2</sup>, Irina Yu. Markovina <sup>3</sup>, Zhaoqing Cong <sup>4</sup>, Siqi Ma <sup>4</sup>, Zhengqi Dong <sup>4</sup>, Feifei Yang <sup>4</sup> and Yonghong Liao <sup>4</sup>

<sup>1</sup> Laboratoty of Nanobiotechnology, Institute of Biomedical Chemistry, Pogodinskaya Str. 10/8, 119121 Moscow, Russia

<sup>2</sup> Nelubin Institute of Pharmacy, Sechenov First Moscow State Medical University, Trubetskaya Str. 8/2, 119991 Moscow, Russia

<sup>3</sup> Institute of Linguistics and Intercultural Communication, Sechenov First Moscow State Medical University, Trubetskaya Str. 8/2, 119991 Moscow, Russia

<sup>4</sup> Institute of Medicinal Plant Development, Chinese Academy of Medical Sciences & Peking Union Medical College, Malianwa North Road 151, Beijing 100193, China

\* Correspondence: terekhov\_r\_p@staff.sechenov.ru; Tel.: +7-499-749-79-91

**Abstract:** Taxifolin is known as an active pharmaceutical ingredient (API) and food supplement due to its high antioxidant activity, multiple pharmacological effects, and good safety profile. Previously, taxifolin spheres (TS) were obtained from industrially produced API taxifolin in Russia (RT). In our work, we perform a pharmaceutical analysis of this new taxifolin material versus RT. TS is an amorphous material; however, it is stable without the polymer carrier, as confirmed by Fourier transform infrared spectroscopy. Both RT and TS demonstrate high safety profiles and are assigned to Class 1 of the Biopharmaceutical Classification System based on the results of experiments with MDCK cells. The water solubility of the new taxifolin form was 2.225 times higher compared with RT. Hausner ratios for RT and TS were 1.421 and 1.219, respectively, while Carr indices were 29.63% and 19.00%, respectively. Additionally, TS demonstrated sustained release from tablets compared with RT: the half-life values of tablets were 14.56 min and 20.63 min for RT and TS, respectively. Thus, TS may be a promising object for developing oral antiseptics in the form of orally dispersed tablets with sustained release patterns because of its anti-inflammatory, -protozoal, and -viral activities.

**Keywords:** taxifolin; spray drying; polymorphism; tablets



**Citation:** Taldaev, A.; Terekhov, R.P.; Selivanova, I.A.; Pankov, D.I.; Anurova, M.N.; Markovina, I.Y.; Cong, Z.; Ma, S.; Dong, Z.; Yang, F.; et al. Modification of Taxifolin Properties by Spray Drying. *Sci. Pharm.* **2022**, *90*, 67. <https://doi.org/10.3390/scipharm90040067>

Academic Editor: William A. Donaldson

Received: 24 September 2022

Accepted: 11 October 2022

Published: 24 October 2022

**Publisher's Note:** MDPI stays neutral with regard to jurisdictional claims in published maps and institutional affiliations.



**Copyright:** © 2022 by the authors. Licensee MDPI, Basel, Switzerland. This article is an open access article distributed under the terms and conditions of the Creative Commons Attribution (CC BY) license (<https://creativecommons.org/licenses/by/4.0/>).

## 1. Introduction

Flavonoids are extremely widespread in the plant kingdom, especially in food, such as citrus fruits [1–3], tea [4,5], and berries [6,7], and in medicinal plants (sea buckthorn [8,9], St. John's wort [10,11], persicaria [12,13], etc.). These natural compounds are secondary plant metabolites [14], and, according to a chemical point of view, they may be defined as derivatives of 1,3-diphenylpropane. Flavonoids are extensively used due to their bioactivity, eco-friendliness, and cost-effectiveness [15].

Recently, more attention has been paid to taxifolin (2,3-dihydro-3,5,7-trihydroxy-2-(3,4-dihydroxyphenyl)-4H-1-benzopyranone-4), also known as dihydroquercetin (Figure 1). This flavanone may be obtained from *Larix* spp. wood and some other natural objects [16–18]. Taxifolin is characterized by high antioxidant activity [19,20] and a considerable safety profile [21]. Its multiple pharmacological effects are associated with an affinity to different biological targets [22], such as the main protease of SARS-CoV-2 [23], Ebola virus proteins [24], epidermal growth factor receptor, phosphatidylinositol 3-kinase [25], etc. Taxifolin also demonstrates wound-healing activity [26,27]. This natural flavanone is approved as a food supplement in the European Union. In Russia, this compound is industrially produced as an active pharmaceutical ingredient (API). Despite its beneficial properties, taxifolin formulation development is limited due to low bioavailability.

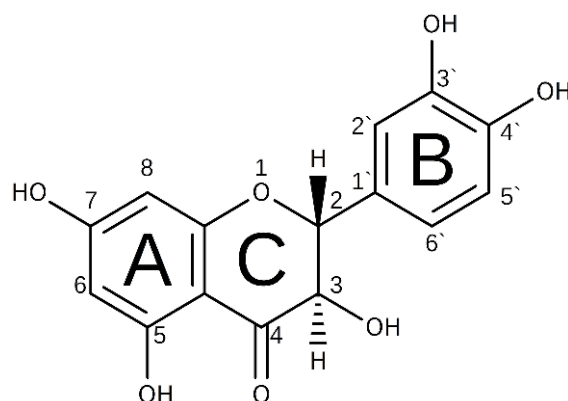


**Figure 1.** Molecular structure of taxifolin.

Poor oral bioavailability and low water solubility at room temperature are common problems related to flavonoid aglycons. One of the most popular solutions for flavonoids is a preformulation by crystal engineering. Crystal engineering is an applied supramolecular chemistry that specializes in the design and synthesis of new solid forms of compounds with targeted properties [26,27]. It can be realized via different approaches, such as sonocrystallization [28], lyophilization [29], grinding [30], and antisolvent precipitation [31]. Patil et al. described an electrospray technique for co-crystallizing quercetin with caffeine and nicotinamide [32]. There are reports about taxifolin chemical modifications [33] and solid dispersion preparation with cyclodextrins [34] and polyvinylpyrrolidone [35]. Liposomal forms of taxifolin were also designed to modulate its bioavailability [36,37]. The new trend in pharmaceutical solids preformulation is a synthesis of amorphous modifications of APIs [38,39].

Spray drying is one of the most commonly used techniques for dried powder production in the pharmaceutical industry [40,41]. This technology has been used as a critical stage of preformulation when manufacturing granulations [42], solid dispersions [43], powder for inhalations [44], microcapsules [45], nanoparticles [46], etc. This tool provides an opportunity to obtain hollow, low-density particles with controlled morphologies and surface properties in particle engineering applications [47]. A considerable number of studies have been published on spray-drying flavonoids. Studies have reported on improvements in water solubility and dissolution rates for quercetin and rutin [48], naringenin [49], hesperidin [50], and naringin [51].

Figure 2 shows taxifolin spheres (TS) that were synthesized without the polymer carrier via spray drying (their morphologies were described in the literature [52]). The results of thermal and X-ray analysis showed the amorphous nature of the new taxifolin form. Changing the solid state may result in increasing the flavonoid's permeability and pharmacological activity [53]. However, the impacts of spray drying on the physicochemical and biopharmaceutical properties of TS have not been researched yet.

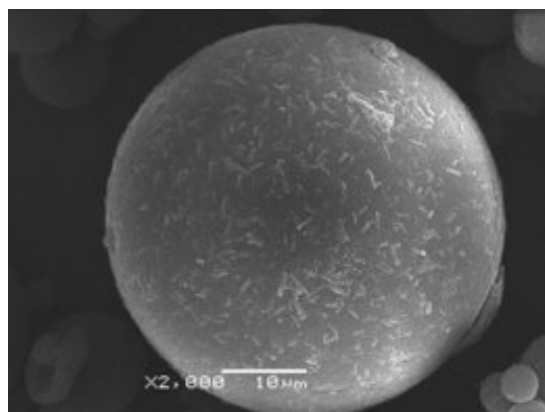


**Figure 2.** Photomicrography of TS.

Therefore, our study objective was to characterize TS using complex pharmaceutical analysis methods.

## 2. Materials and Methods

### 2.1. Materials

The taxifolin substance, which is hereafter referred to as raw taxifolin (RT), was provided by Ametis JSC (Blagoveshchensk, Russia). We used saccharose (Sudzucker AG, Mannheim, Germany), mannitol (Roquette, Lestrem, France), sorbitol (Roquette, Lestrem, France), sodium starch glycolate (JRS Pharma, Rosenberg, Germany), crospovidone (ISP Inc., Wayne, NJ, USA), calcium stearate (LDKkim JSC, Staraya Kupavna, Russia), aspartame (Carl Roth GmbH, Karlsruhe, Germany), and menthol (Carl Roth GmbH, Karlsruhe, Germany) for tablet formation. The solvents, including acetonitrile (Merck, Darmstadt, Germany), denaturated ethanol (Carl Roth GmbH, Karlsruhe, Germany) and formic acid (DikmaPure, Beijing, China), were HPLC-grade, and we obtained water from a Milli-Q water purification system (Millipore, Burlington, MA, USA). Additionally, a standard sample of dihydroquercetin (99.99%; Ametis JSC, Blagoveshchensk, Russia) was used in HPLC analysis.

Dulbecco's modified Eagle's medium (DMEM) with L-glutamine (1X, Corning, Corning, NY, USA), supplemented with 10% fetal bovine serum (FBS; 1X, Gibco, Waltham, MA, USA) and a solution of penicillin and streptomycin (P/S; 1X, Gibco, Waltham, MA, USA) in a ration volume of 89:10:1 served as a medium during the ex vivo experiment. We used dimethyl sulfoxide (DMSO; 99.5%; XiLonhScienitifific, Guangzhou, China) and the Cell Counting Kit (CCK-8; Beijing Bio Dee Biotechnologies, Beijing, China) in the modified MTT test. Hank's balanced salt solution (HBSS; 1X) was purchased from Gibco (Waltham, MA, USA).

### 2.2. Spray Drying of Taxifolin

We based TS preparation technology on the modified preparation of milk powder. RT (1 kg) was dissolved in water (40 L) at 60 °C with constant stirring, which was possible because of taxifolin's high solubility in hot water. We used GLP-60 centrifugal sprat with a high-speed blade disk at the inlet and outlet air temperatures of 180 °C and 80 °C, respectively. We kept taxifolin in the dryer chamber for 1.5–2.0 s. The relative centrifugal force (RCF) of the disk atomizer was  $22,700 \times g$ . This sample hereafter is referred to as TS. The spray drying yield ranged from 95.4% to 98.8%.

### 2.3. Tablet Preparation

We prepared the taxifolin tablets for the dissolution test by direct compression using a lab mechanical press. The total tablet weights ranged from 100 mg to 300 mg. Table 1 presents the mass ratio of TS and inactive ingredients that are widely used in orally dispersed tablets [54]. The pressure was 7 atm, and we controlled it via integral dynamometer. The tablet series for the comparative analysis of taxifolin forms were prepared with TS and RT.

### 2.4. Cell Culture

The Madin–Darby Canine Kidney (MDCK) cell line was obtained from the Cell Culture Centre of Chinese Academy of Medical Sciences (Beijing, China). This cell model is accepted by the FDA for biopharmaceutical assays as an alternative for widely used Caco-2 cells [55]. The advantage of using MDCK cells is that they quickly integrate the monolayer.

We grew cells in plastic culture flasks in cultural medium at 37 °C in a humidified atmosphere of 5% CO<sub>2</sub>. The medium was changed every two days. The cells were routinely maintained by regular passing. The cells used for ex vivo experiments were between passage numbers 25 and 30.

**Table 1.** Formulations of taxifolin tablets.

No	Mass of Tablet, mg	TS	Mass of Component, mg							
			Saccharose	Mannitol	Sorbitol	Sodium Starch Glycolate	Crospovidone	Calcium Stearate	Aspartame	Menthol
1	150.0	20.0	-	125.0	-	3.0	-	2.0	-	-
2	150.0	20.0	-	125.0	-	-	3.0	2.0	-	-
3	150.0	20.0	125.0	-	-	3.0	-	2.0	-	-
4	150.0	20.0	125.0	-	-	-	3.0	2.0	-	-
5	150.0	20.0	-	-	125.0	3.0	-	2.0	-	-
6	150.0	20.0	-	-	125.0	-	3.0	2.0	-	-
7	150.0	20.0	-	120.0	-	3.0	-	2.0	-	-
8	150.0	20.0	-	120.0	-	-	3.0	2.0	-	-
9	150.0	20.0	125.0	-	-	3.0	-	2.0	-	-
10	150.0	20.0	125.0	-	-	-	3.0	2.0	-	-
11	150.0	20.0	-	-	120.0	3.0	-	2.0	-	-
12	150.0	20.0	-	-	120.0	-	3.0	2.0	-	-
13	150.0	20.0	-	120.0	-	-	3.0	2.0	5.0	-
14	150.0	20.0	110.0	-	-	-	8.0	2.0	5.0	5.0
15	150.0	20.0	125.0	-	-	-	8.0	2.0	5.0	-
16	150.0	20.0	-	120.0	-	-	3.0	2.0	-	5.0
17	150.0	20.0	115.0	-	-	-	8.0	2.0	-	5.0
18	300.0	20.0	-	270.0	-	-	3.0	2.0	-	5.0
19	300.0	20.0	265.0	-	-	-	8.0	2.0	-	5.0

### 2.5. Antimicrobial Activity

The antimicrobial activity of taxifolin samples was analyzed in vitro using the agar diffusion method in biphasic medium, which is generally accepted in biomedical science [56,57]. At first, we placed 10 mL of agar medium (pH value between 6.8 and 7.0) in Petri dishes. We added an equal amount of Hottinger's agar after the solidification of the lower layer. We prepared the medium in wells when the top layer was cooled; the inner diameters were  $8.0 \pm 0.1$  mm, and the heights were  $5.0 \pm 0.1$  mm. We filled them with different taxifolin sample solutions in DMSO (10%) with 0.01 mg/mL concentration. The pure DMSO was used as a negative control.

We used the following reference strains as test cultures: *Staphylococcus aureus* (ATCC 6538), *Escherichia coli* (M 17), *Micrococcus luteus* (ATCC 10240), and *Bacillus cereus* (IP 5832). The microbial load was 107 colony-forming units per 1 mL of nutrient medium (CFU/mL). Petri dishes were incubated for 20 h at 37 °C.

We measured microbial growth inhibition zones to assess the antimicrobial activity. Measurements were accurate to 1 mm. Each sample was analyzed 3 times with every test culture.

### 2.6. Fourier Transform Infrared Spectroscopy (FTIR)

We prepared KBr discs containing 0.02 mg of taxifolin samples separately. FTIR spectra were recorded from  $4000\text{ cm}^{-1}$  to  $350\text{ cm}^{-1}$  with Fourier transform infrared spectrometer FSM-1201 (Infraspek, Saint Petersburg, Russia). The resolution was  $1\text{ cm}^{-1}$ . We used blank KBr discs as a reference sample.

### 2.7. Solubility

We analyzed the water solubility of the taxifolin samples according to the European Pharmacopoeia 10.0 [57]. First, we added 1.0 g of the substance to 1.0 mL of solvent; then, we shook the mixture continuously for 10 min at 20 °C. If the substance fully dissolved, we determined it to be very soluble. We considered a substance to be dissolved if no particles could be seen when examined against light. If the substance did not fully dissolve, we added 1.0 mL of solvent to 100 mg of the substance and performed the dissolution as described above. If the substance fully dissolved, it was determined to be freely soluble. If the substance did not fully dissolve, we added 2.0 mL of solvent and continued dissolution. If the substance fully dissolved, it was considered soluble. If the substance did not fully dissolve, we added 7.0 mL of solvent and continued dissolution. If the substance fully dissolved, it was considered sparingly soluble. If the substance did not fully dissolve, we added 10.0 mL of solvent to 10.0 mg of substance and performed dissolution as described above. If the substance fully

dissolved, it was considered slightly soluble. If the substance did not fully dissolve, we added 100 mL of solvent to 10.0 mg of substance and performed dissolution as described above. If the substance fully dissolved, it was considered very slightly soluble, and if the substance did not dissolve, then it was considered practically insoluble.

We also determined the exact solubility value. We added samples equivalent to 40 mg of taxifolin to 10 mL of water and shook the mixture continuously for 5 min. The suspension was divided into 5 Eppendorf tubes (2 mL). We used one of the tubes as a zero point. We shook another 4 samples for 1, 2, 4, and 6 h using Mixer 5432 (Eppendorf, Hamburg, Germany) worked at 1450 rpm. All stock solutions were centrifuged for 5 min at  $\text{RCF } 18,300 \times g$  by Centrifuge 5413 (Eppendorf, Hamburg, Germany). The supernatant (50  $\mu\text{L}$ ) was diluted in 9.95 mL of water. We determined the taxifolin concentrations of these solutions via UV spectrometry using a calibration curve in the range 0.5–2.5 mg/mL. We used water as a reference sample. We performed each test in triplicate. A Cary-100 UV/Vis spectrophotometer (Varian, Palo Alto, CA, USA) was operated at 290 nm for maximum taxifolin absorption in ethanol. We validated this method, and it was characterized by appropriate values of linearity ( $r^2 = 0.9960$ ), trueness, and precision. The standard deviations of the analytical signal lie in the range from 0.0474 to 0.0936. The free term (0.0351) does not significantly differ from zero.

## 2.8. Cell Viability Test

We determined the cytotoxicity of the taxifolin samples using the CCK-8 method. MDCK cells in complete medium were seeded on 96-well plates at a final density of  $4 \times 10^4$  cells/well. We removed the medium after 36 h and incubated the cells for 2 h with taxifolin samples of different concentrations (0.01, 0.03, 0.06, 0.12, 0.25, 0.50, 1.00, and 2.00 mg/mL). DMSO and pure DMEM were used as a positive and negative control, respectively. Then, we removed the surfactants and added CCK-8 for 2 h incubation. The absorbances were measured 6 times at 450 nm using SPARK (Tecan Group Ltd., Zürich, Switzerland) for the concentration of each sample. We calculated the viability ( $V$ ) as (1):

$$V = \frac{A_n - A_0}{A_{100} - 0A_0} \times 100\%, \quad (1)$$

where  $A_n$  is a mean absorbance of CCK-8 solutions after incubation with MDCK cells contacted with taxifolin samples,  $A_0$  is a mean absorbance of CCK-8 solutions at the negative control, and  $A_{100}$  is a mean absorbance of CCK-8 solutions at the positive control.

## 2.9. Permeability Assay

MDCK cells were seeded into a 12-well plate at a final density of  $2 \times 10^6$  cells/well. We used the transepithelial electrical resistance (TEER) value to monitor the integrity of the monolayer. We employed a monolayer with a TEER value higher than  $300 \Omega \cdot \text{cm}^2$  in the experiment.

The solutions of taxifolin in DMEM (0.5 mL) with a concentration of 1 mg/mL were added to an apical side. We placed the warmed HBSS (1.5 mL) into a basolateral side. We took aliquots of 0.5 mL from the receiver chamber at different time intervals (15, 30, 60, 90, and 120 min) after 4 periods of incubation for each time point. After each sampling, an equal volume of blank HBSS was added in the receiver chamber to maintain a constant volume.

We determined the concentrations of taxifolin in aliquots via HPLC-UV using a standard curve in the range of 0.01–100.00  $\mu\text{g/mL}$ . All samples were twice diluted by acetonitrile and centrifugated for 5 min at  $\text{RCF } 27,950 \times g$ . We injected the supernatant (20  $\mu\text{L}$ ) into the HPLC system for the assay. Each test was performed in triplicate. A Waters 600 HPLC pump with a Waters 2489 UV/Visible detector was employed to separate the compounds through a reversed-phase column (Phenomenex Luna, C-18, 2.1 mm  $\times$  250 mm, 5  $\mu\text{m}$ ) at a flow rate of 1 mL/min. The mobile phase consisted of acetonitrile (30%) and 0.1% acetic acid in water (70%). The wavelength for UV detection was 290 nm, and the column temperature was set at 25  $^\circ\text{C}$ . We identified taxifolin by comparing the retention time of a standard sample and quantified it through calculating the area under the curve with the

external standard. So, this method may be considered specific. It also demonstrates suitable validation parameter values. The linearity was quite high ( $r^2 = 0.9999$ ). The standard deviations of the analytical signal vary in the range from 27,254.8 to 265,827.9. The free term (5296.4) does not statistically significantly differ from zero.

We calculated the apparent permeability coefficient ( $P_{app}$ ) using Equation (2):

$$P_{app} = \frac{\frac{dC}{dT} \times V}{A \times C}, \quad (2)$$

where  $dC/dT$  is the change in taxifolin concentration in the receiver chamber over time,  $V$  is the volume of the solution in receiver chamber,  $A$  is the membrane surface area of the MDCK cell monolayer ( $4.7 \text{ cm}^2$ ), and  $C$  is the loaded taxifolin concentration in the donor chamber.

#### 2.10. Flowability

We measured the angle of repose and compressibility to characterize the taxifolin powder's flowability.

We determined the repose angle using a flow tester GTL (Erweka GmbH, Langen, Germany) with a 10 cm-diameter base plate. Samples of both taxifolin forms (100 g) were discharged from a hole with an inner diameter of 25 mm while maintaining free fall. The test was performed in triplicate for each sample. We analyzed the results according to European Pharmacopoeia 10.0 [58].

We determined compressibility using a tap density tester SVM 121 (Erweka GmbH, Langen, Germany). We gently filled a 150 mL graduated cylinder with 100 mL of sample and weighed it to calculate the bulk density ( $BD$ ). Then, the cylinder containing the sample was tapped until the volume stopped changing (1250 times), allowing us to measure the tapped density ( $TD$ ). The test was performed in triplicate for each sample.

We calculated the Hausner ratio ( $HR$ ) and Carr index ( $CI$ ) from compressibility data using Equations (3) and (4), respectively:

$$HR = TD/BD, \quad (3)$$

$$CI = ((1 - BD)/TD) \times 100\%. \quad (4)$$

#### 2.11. Disintegration of Tablets

We determined the disintegration time using a ZT 121 light tester (Erweka GmbH, Langen, Germany). The analysis was performed in distilled water ( $1.0 \text{ L}$ ) at  $37 \pm 2^\circ\text{C}$ . A sample set consisted of 6 tablets for each sample.

#### 2.12. Tablet Hardness

We determined tablets' hardness with the TBH 100 tester (Erweka GmbH, Langen, Germany) using a set of 10 tablets for each sample.

#### 2.13. Friability Test

We determined the friability of tablets based on different taxifolin samples using a TAR 220 friabilator (Erweka GmbH, Langen, Germany). We individually weighed a set of 10 tablets with 1.0 mg accuracy for each sample before loading them into the friabilator for 100 drops (25 rpm over a period of 4 min). The percentage weight loss was calculated for individual tablets (% friability) based on the weight measurements after the friability test. We carefully removed particles on the tablet surface with a soft brush before weighing.

#### 2.14. Dissolution Test

We performed the paddle method using a DT-600 dissolution tester (Erweka, Germany) at the HBSS with 6 tablets in different taxifolin forms, which were placed in individual receiver chambers. The volume of solvent was 500 mL, the temperature was  $37 \pm 0.5^\circ\text{C}$ , and the speed of rotation was 50 rpm. Aliquots of 5.0 mL were taken from the receiver



chamber at different time intervals (5, 10, 20, 30, and 45 min) after loading 5 times for each time point. We added an equal volume of blank HBSS in the receiver chamber after each sampling to maintain a constant volume.

We determined the concentrations of taxifolin in aliquots via UV spectrometry using a calibration curve in the range 5.0–25.0 µg/mL. Each test was performed in triplicate. Cary-100 (Varian, Palo Alto, CA, USA) was operated at 324 nm in consideration of maximum taxifolin absorption in the phosphate buffer. We tested this method using several validation parameters. We considered the appropriate linearity according to  $r^2 = 0.9994$ . The trueness was evaluated by comparing the free term of the calibration curve equation and the confidence interval in three concentrations. The standard deviations of the analytical signal were between 0.0637 and 0.1035. The free term (0.0533) did not differ significantly compared with zero.

We calculated the release constant ( $K$ ) and half-life values ( $T_{50\%}$ ) as (5) and (6), respectively, to characterize the dissolution profiles of taxifolin samples:

$$K = \frac{\ln\left(\frac{C_0}{C_0 - C_t}\right)}{t}, \quad (5)$$

$$T_{50\%} = \ln \frac{2}{K}, \quad (6)$$

where  $C_0$  is the initial taxifolin concentration in a tablet and  $C_t$  is a taxifolin concentration in a solution at the moment  $t$ .

We calculated the difference ( $f_1$ ) and similarity factors ( $f_2$ ) as (7) and (8), respectively, to perform a quantitative analysis of dissolution profiles of tablets of different taxifolin samples:

$$f_1 = \frac{\sum_{t=1}^n |R_t - T_t|}{\sum_{t=1}^n R_t} \cdot 100\%, \quad (7)$$

$$f_2 = 50 \cdot \log \left( \sqrt{1 + \frac{\sum_{t=1}^n (R_t - T_t)^2}{n}} \cdot 100 \right), \quad (8)$$

where  $n$  is the number of dissolution intervals,  $R_t$  is the release results (%) of the tablets on RT basis at time point  $t$ , and  $T_t$  is the release results (%) of the tablets on a TS basis at time  $t$ .

### 2.15. Statistical Analysis

All data were analyzed using Microsoft Excel (version 16.0; Microsoft, Albuquerque, NM, USA). We present the results as means  $\pm$  SEM for solubility, permeability assay, disintegration time, tablet hardness, and dissolution test. Each viability value represents the mean of six independent, parallel wells.

The statistical significance of the antimicrobial activity assessment was determined using the Mann–Whitney  $U$  test [59,60]. We calculated the  $U$  value using Equation (9):

$$U = n_1 n_2 + \frac{n_x(n_x + 1)}{2} - T_x, \quad (9)$$

where  $n_1$  is the size of the RT group,  $n_2$  is the size of the TS sample,  $n_x$  is the size of the largest sample, and  $T_x$  is the sum of the largest sample ranks. We assessed the results according to the appropriate table.

## 3. Results

### 3.1. FTIR Spectroscopy

We investigated the possibility of a chemical reaction during spray drying using FTIR analysis (Figure 3). The taxifolin samples' FTIR spectra showed a broad absorption band of the –OH stretching vibration with a maximum at  $\sim 3400 \text{ cm}^{-1}$ , an intensive band of  $>\text{C}=\text{O}$  at  $\sim 1600 \text{ cm}^{-1}$ , a band of bending –OH at  $\sim 1350 \text{ cm}^{-1}$ , and a band of –C–O–C– stretching

vibration at  $\sim 1250\text{ cm}^{-1}$ . Based on these data, we assume that there was no chemical structure transformation during the TS formation.

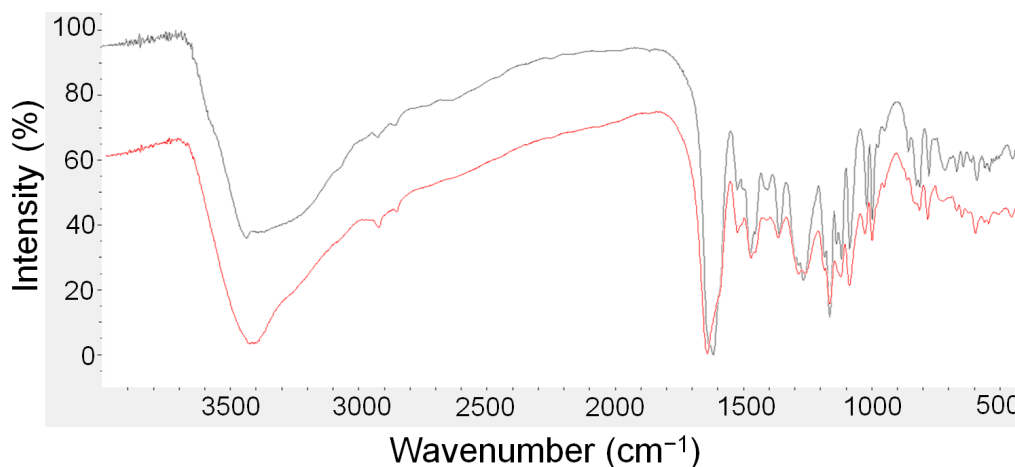


**Figure 3.** FTIR spectra of RT (black) and TS (red).

However, a more careful analysis of IR data shows that there are some differences for different taxifolin samples. TS spectra were characterized by strong absorption bands. The RT IR spectrum in the same region exhibited a smooth broad band at  $3550\text{--}3200\text{ cm}^{-1}$ , indicative of intermolecular H-bonds involving hydroxyls. Furthermore, the carbonyl functional group's absorption band in the IR spectrum moved from  $1623.88\text{ cm}^{-1}$  to  $1643.18\text{ cm}^{-1}$ . Additionally, there were slight differences in the fingerprint area, which is apparently a result of the phase transition. The RT IR spectrum contained two thin absorption bands at  $\sim 1000\text{ cm}^{-1}$  and two absorption bands at  $\sim 750\text{ cm}^{-1}$  in the fingerprint area. At the same time, the TS spectrum demonstrated more wide bands at  $\sim 1000\text{ cm}^{-1}$  and only one band at  $750\text{ cm}^{-1}$ . The intensity of the RT absorption bands decreased at  $700\text{--}600\text{ cm}^{-1}$ , while the intensity in the TS spectrum increased.

### 3.2. Solubility

RT is considered a *very slightly soluble* substance according to the European Pharmacopoeia 10.0, which means its solubility is between  $0.1\text{ mg/mL}$  and  $1.0\text{ mg/mL}$ . TS's solubility increased, and we found this form to be *slightly soluble* according to the European Pharmacopoeia 10.0 (between  $1.0\text{ mg/mL}$  and  $10.0\text{ mg/mL}$ ) [58].

We also identified the exact solubility of taxifolin samples. The concentration curve forms a plateau for both samples after 6 h (Table 2). The solubility of RT and TS was  $0.9557 \pm 0.0230\text{ mg/mL}$  and  $2.1265 \pm 0.2289\text{ mg/mL}$ , respectively.

**Table 2.** Correlation between concentration of taxifolin and duration of its dissolution.

Sample	Taxifolin Concentration, mg/mL				
	0 h	1 h	2 h	4 h	6 h
RT	$0.700 \pm 0.016$	$0.764 \pm 0.017$	$0.785 \pm 0.018$	$0.884 \pm 0.020$	$0.956 \pm 0.023$
TS	$1.642 \pm 0.177$	$1.764 \pm 0.180$	$1.822 \pm 0.196$	$2.099 \pm 0.226$	$2.127 \pm 0.229$

We observed precipitation after 24 h of storing the spray-dried taxifolin solution.

### 3.3. Antimicrobial Activity

We measured the cultures' growth test inhibition zones in comparison with the negative control to assess the taxifolin samples' antimicrobial activity (Table 3). The  $U$  values in growth inhibition zones for *S. aureus*, *E. coli*, *M. Luteus*, and *B. cereus* were 1.5, 3.0, 3.0, and 1.5, respectively. The  $U$  value must be less than 0 ( $p = 0.05$ ) for the significance to be



estimated. So, we did not observe significant differences in the antimicrobial activity of the taxifolin samples, and both may be characterized as moderate.

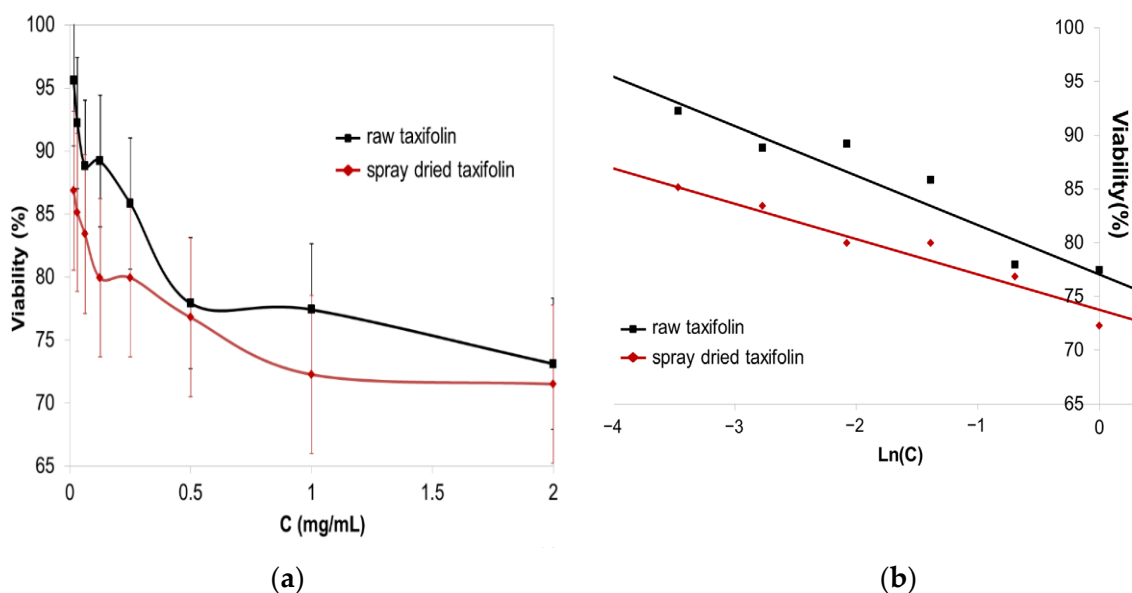
**Table 3.** Antimicrobial activity of taxifolin samples.

Sample	Growth Inhibition Zone, mm			
	<i>Staphylococcus aureus</i>	<i>Escherichia coli</i>	<i>Micrococcus luteus</i>	<i>Bacillus cereus</i>
RT	13.67 ± 0.58	14.00 ± 1.00	14.00 ± 0.00	14.33 ± 0.58
TS	13.00 ± 0.00	13.33 ± 1.15	13.67 ± 0.58	14.00 ± 0.00

### 3.4. Cell Viability Test

It was necessary to determine the toxicity of the taxifolin samples for the MDCK cell model before performing the permeability assay.

Figure 4a shows the dose-dependent toxicity of the taxifolin samples. High cell viabilities were confirmed in both RT and TS at high concentrations. We did not observe significant differences in cell viability between the taxifolin samples. However, the cell viability for both samples was limited to about 75%.



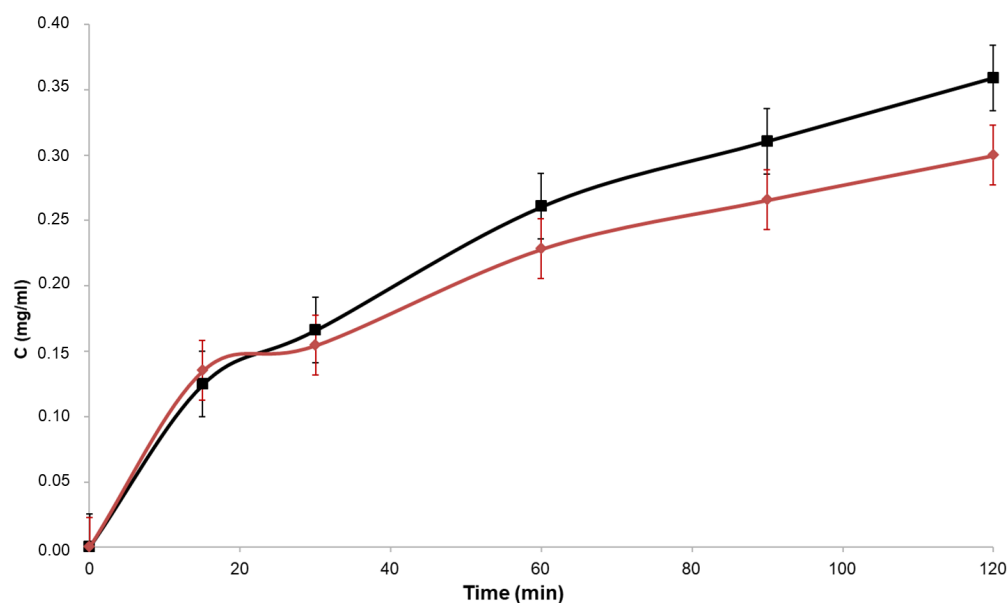
**Figure 4.** Effect of concentrations on cytotoxicity of RT (black) and TS (red): (a) at natural scale of concentration; (b) at logarithmic scale.

Figure 4b shows the logarithmic correlations between the concentrations of the taxifolin samples and cytotoxicity. The correlation coefficients for crystal taxifolin and spray-dried taxifolin were 0.9544 and 0.9710, respectively. The nonlinear dose dependence may be explained by taxifolin's low water solubility. We obtained the suspension at higher concentrations; therefore, the decrease in viability was caused not only by the dissolved molecules but also by the physical impacts of solid taxifolin particles.

Figure 4 shows the viability of MDCK cells was acceptable for both samples, which meant we could use this cell model for the permeability assay.

### 3.5. Permeability Assay

The next stage of our research was the infinity permeability assay (Figure 5). After the first 90 min, there was no significant difference in flavonoid concentration in the receiver solution. Surprisingly, the concentration of taxifolin in the RT receiver solution was higher compared with TS after 2 h. In general, the apparent permeability coefficients were  $14.8 \times 10^{-6} \pm 0.349$  cm/s and  $10.7 \times 10^{-6} \pm 0.253$  cm/s for RT and TS, respectively.



**Figure 5.** Dynamic of taxifolin concentration in receiver solution during permeability assay for RT (black) and TS (red).

We also measured the TEER values of the MDCK monolayers in both samples to confirm the high viability of the cell models. The viability values were  $70.75 \pm 9.86\%$  and  $86.82 \pm 5.53\%$  for RT and TS, respectively. Therefore, there was a significant difference between taxifolin samples, and TS demonstrated a slightly higher safety profile.

### 3.6. Flowability

We performed a flowability analysis of taxifolin samples via two independent methods using repose angles and compressibility.

The repose angles' mean values were  $46.8^\circ \pm 4.7^\circ$  and  $29.6^\circ \pm 7.9^\circ$  for RT and TS, respectively. Based on these results, the RT flowability may be considered poor according to the European Pharmacopoeia 10.0; however, TS demonstrates a fair flowability [58].

We used the compressibility data to calculate the *HR* and *CI* (Table 4). Our results confirm that TS is characterized by better flowability and, while primary, may be considered more preferable for the pharmaceutical formulation.

**Table 4.** Flowability characteristics of taxifolin samples.

Sample	<i>HR</i>	<i>CI</i> , %	Flow Description
RT	$1.421 \pm 0.149$	$29.63 \pm 3.11$	poor
TS	$1.219 \pm 0.113$	$19.00 \pm 1.77$	fair

### 3.7. Design of Orally Dispersed Tablets with TS

Our taxifolin tablet design was based on previous clinical and preclinical research of this bioflavonoid. Shkarenkov et al. showed the safety of a 20 mg taxifolin dose in rats during preclinical studies [61]; furthermore, Kolikhir et al. confirmed its effectiveness [62]. Later, this dose showed clinical significance in a treatment of acute pneumonia [63]. According to the data, a single dose of taxifolin is 20 mg per tablet, and it was noted that the amount of antifriction material should be no more than 1% [58]. We required taste-making agents, such as aspartame and menthol, because of taxifolin's bitter taste.

We assessed the tablet samples and performed the selection of the optimal formulation on the basis of the following tablets characteristics: disintegration time, hardness, and taste (Table 5). We did not perform the hardness analysis if the disintegration time was not appropriate, and we assessed the formulation's taste with suitable technological parameters.

Sample 19 demonstrates the best set of characteristics; therefore, we selected it for a future comparative study of RT and ST.

**Table 5.** Selection parameters of TS-based tablet formulation.

No.	Disintegration Time, min		Hardness, N		Taste
	Measurement	Regulatory Requirements	Measurement	Regulatory Requirements	
1	9.3 ± 0.6	[15.0–45.0]	-	>40.0	-
2	13.8 ± 0.9		-		-
3	4.4 ± 0.3		-		-
4	4.7 ± 0.3		-		-
5	7.3 ± 0.5		-		-
6	4.9 ± 0.3		-		-
7	1.3 ± 0.1		-		-
8	7.3 ± 0.5		-		-
9	9.8 ± 0.6		-		-
10	18.1 ± 1.1		71.9 ± 20.8		bittersweet, astringent
11	3.8 ± 0.4		-		-
12	6.2 ± 2.3		-		-
13	39.9 ± 2.5		22.2 ± 6.4		-
14	17.0 ± 1.1		25.1 ± 7.3		-
15	23.1 ± 1.5		26.0 ± 7.5		-
16	10.1 ± 0.6		-		-
17	40.2 ± 2.3		34.5 ± 10.0		-
18	8.0 ± 0.5		-		-
19	36.4 ± 2.3		81.0 ± 23.4		cooling, spicy

### 3.8. Characteristics of Tablets

Considerable differences in hardness and friability between tablets obtained with different taxifolin samples were observed (Table 6). Both tablet series manufactured with RT and TS demonstrated acceptable results according to the European Pharmacopoeia 10.0 [58].

**Table 6.** Strength characteristics of taxifolin tablets.

Sample	Hardness, N		Friability, %	
	Measurement	Regulatory Requirements	Measurement	Regulatory Requirements
RT	74.9 ± 33.6	>40.0	0.3	<3.0
TS	81.0 ± 23.4		1.3	

However, we observed a significant difference in disintegration time for different tablet samples. Tablets based on RT disintegrated for  $7.1 \pm 1.8$  min, while for samples with TS, this characteristic was five times higher at  $36.4 \pm 2.3$  min.

### 3.9. Dissolution Test

Figure 6 shows taxifolin's in vitro dissolution profiles. After 45 min, 88.3% of RT was released, and the release ratio for TS was 77.9%. We noticed that at 5 min, TS demonstrated a three-times-higher release ratio than RT.

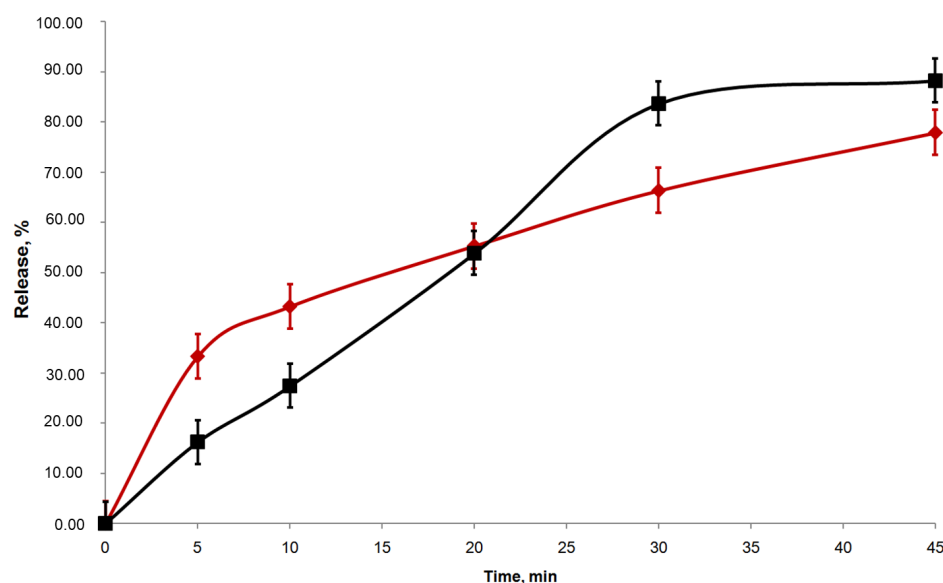


**Figure 6.** Dissolution profiles of RT (black) and TS (red).

We calculated the parameters of taxifolin release based on the tablets' dissolution profiles (Table 7). All calculated characteristics demonstrate significant differences between the two groups of tablets.

**Table 7.** Release parameters of taxifolin tablets.

Sample	Parameters of Release Kinetic		$f_1$	$f_2$
	$K, \text{min}^{-1}$	$T_{50\%}, \text{min}$		
RT	$0.034 \pm 0.002$	$20.63 \pm 1.13$	$23.0 \pm 1.7$	$42.8 \pm 6.0$
TS	$0.048 \pm 0.002$	$14.56 \pm 0.48$		

Therefore, the spray-dried processing of taxifolin results in a sustained release of this flavonoid. We noticed that the dissolution test data correlated with the permeability assay results.

#### 4. Discussion

We designed our project to research the pharmaceutical characteristics of TS and to determine the effects of spray drying on taxifolin.

Based on IR spectroscopy patterns, we determined that there was no change in the chemical structure of taxifolin during spray drying. Our results correlate with previous data obtained using UV spectroscopy, NMR  $^1\text{H}$ , and mass spectrometry [52]. However, we observed some differences in IR spectra that may be explained by phase transition, especially in the fingerprint area, which apparently correlates with the out-of-plane vibrations of  $-\text{CH}$ . Therefore, the changing physical–chemical and pharmaceutical properties are associated with crystal-to-amorphous phase transitions. We also discovered that TS is stable at the standard conditions without the polymer carrier according to IR spectroscopy, which is a key difference when compared with the earlier obtained solid dispersions [34,35].

Taxifolin demonstrates a high safety profile [21,64]. Moreover, our experiment did not detect any increase in cytotoxicity after spray drying. Furthermore, the viability of MDCK cells was about 75% for both taxifolin samples and, based on the TEER value measurement data, we suggest that TS is characterized by a higher safety profile.

We performed the MTT test to analyze the accessibility of MDCK cells for a permeability analysis of taxifolin samples. Permeability and solubility are key characteristics in the API classification according to the Biopharmaceutical Classification System (BCS). The BCS defines “high solubility” as the dissolution of a maximal single dose (MSD) in 250 mL of

water. Diquertin<sup>®</sup> is the only remedy regarding taxifolin (characterized by MSD 60 mg) [63]. Therefore, both RT and TS taxifolin samples are characterized by high solubility according to the BCS. Permeability is considered high if the apparent permeability coefficients are higher than for the compound with known high permeability, such as metoprolol. According to the data found in the literature, the apparent permeability of metoprolol in a weak acid medium is  $7.8 \times 10^{-6}$  cm/s [65,66]. Therefore, both taxifolin samples demonstrated high permeability and may belong to Class 1 of the BCS.

Different researchers reported on taxifolin's poor water solubility. According to the literature, this parameter ranges from 0.87 mg/mL to 0.96 mg/mL [34,67]. Our results are supported by these data (we found the solubility of RT was 0.9557 mg/mL). Furthermore, Zu et al. and Potoroko et al. reported a 0.004 mg/mL and 0.002 mg/mL taxifolin solubility, respectively [68,69]. The main purpose of taxifolin phase modification via spray drying is to improve its water solubility at room temperature. We observed a significant 2.225-times increase in TS water solubility compared with RT. The differences in the physical–chemical properties of the taxifolin samples may be associated with the “spring and parachute” effect, which is common in crystal engineering [26,70]. However, during the TS dissolution process, metastable supramolecular complexes of taxifolin with solvent molecules form, resulting in an increase in water solubility (spring effect). However, these complexes are not stable, and taxifolin precipitation will occur. The stability of supramolecular complexes (parachute effect) should be taken into account during pharmaceutical formation.

We observed an extensive increase in taxifolin concentration in TS after the first few minutes of the permeability assay and dissolution test, which may be associated with the spring effect. However, the intensity of the concentration increases later decreased in both analyses, possibly because of the destruction of metastable supramolecular complexes of taxifolin with solvent molecules. Our results contribute to drug development in at least two major respects. First, they prove the therapeutic dose of taxifolin can be reached in a short amount of time, which is vital for topical action remedies because this results in faster estimations of pharmacological effects. Second, the following slow release may maintain taxifolin concentrations, and the half-life value of amorphous taxifolin was 29.4% higher. The advantages of such a dissolution profile have already observed for the cocrystals of other flavonoids [71–73].

Prior studies have noted the moderate antimicrobial activity of taxifolin [74–76]; however, it is not high enough to consider this compound as an antibiotic. Despite this, taxifolin can find applications in antiseptic remedies. Its observed antimicrobial effects may be explained by the inhibition of essential bacterial proteins, such as enoyl-acyl carrier protein reductase [77]; however, we detected no polymorphism impacts on the bactericidal and bacteriostatic properties of taxifolin. We did not observe any differences between RT and TS in this parameter. The reason for this might be explained by our study design: the incubation time was much higher than the lifetime of the supramolecular complexes after TS dissolution; therefore, the effect of increased solubility was minimized.

The results of our study show that TS may be a promising object for the development of an oral antiseptic in the form of orally dispersed tablets with sustained release patterns because of its anti-inflammatory [78], -protozoal [79], and -viral [23,24] activities. Abdulrazzak et al. previously developed oral taxifolin tablets [80]; however, they are based on RT. Fair flowability, acceptable hardness and friability, and long disintegration times are the advantages of TS compared with RT.

Optimizing the phase state for APIs is a new stage of drug development. Researchers are paying increasing amounts of attention to amorphous solids because they demonstrate numerous advantages compared with initial crystal forms [81,82]. Our results concur with those of previous studies. To further explore the possibility of using spray drying on taxifolin, additional studies will be needed to determine the influence of the phase state of this bioflavonoid on its therapeutic efficacy.

## 5. Conclusions

TS is a new taxifolin modification obtained via spray drying. It is stable without the polymer carrier, so TS may be beneficial from a drug loading perspective. This substance demonstrates higher water solubility, a high safety profile, fair flowability, and a sustained dissolution profile. Thus, spray drying can be used for preformulation of taxifolin to obtain an API for manufacturing an oral antiseptic in the form of orally dispersed tablets with a sustained release pattern.

**Author Contributions:** Conceptualization, I.A.S.; methodology, R.P.T., D.I.P., Z.C., S.M., Z.D. and F.Y.; software, A.T.; validation, D.I.P.; formal analysis, D.I.P.; investigation, R.P.T. and D.I.P.; resources, A.T.; data curation, R.P.T. and I.Y.M.; writing—original draft preparation, R.P.T. and I.Y.M.; writing—review and editing, I.A.S., M.N.A., Z.C., F.Y., Y.L. and I.Y.M.; visualization, A.T.; supervision, I.A.S., M.N.A. and Y.L.; project administration, R.P.T.; funding acquisition, A.T. All authors have read and agreed to the published version of the manuscript.

**Funding:** This work was financed by the Ministry of Science and Higher Education of the Russian Federation within the framework of state support for the creation and development of World-Class Research Centers “Digital Biodesign and Personalized Healthcare” (No. 75-15-2022-305).

**Institutional Review Board Statement:** Not applicable.

**Informed Consent Statement:** Not applicable.

**Data Availability Statement:** Not applicable.

**Acknowledgments:** We would like to thank N.A. Tyukavkina for her constructive advice.

**Conflicts of Interest:** The authors declare no conflict of interest.

## References

- Deng, M.; Dong, L.; Jia, X.; Huang, F.; Chi, J.; Muhammad, Z.; Ma, Q.; Zhao, D.; Zhang, M.; Zhang, R. The flavonoid profiles in the pulp of different pomelo (*Citrus grandis* L. Osbeck) and grapefruit (*Citrus paradise* Mcfad) cultivars and their in vitro bioactivity. *Food Chem. X* **2022**, *15*, 100368. [\[CrossRef\]](#) [\[PubMed\]](#)
- Zhao, C.; Wang, F.; Lian, Y.; Xiao, H.; Zheng, J. Biosynthesis of citrus flavonoids and their health effects. *Crit. Rev. Food SciNutr.* **2020**, *60*, 566–583. [\[CrossRef\]](#)
- Wang, S.; Yang, C.; Tu, H.; Zhou, J.; Liu, X.; Cheng, Y.; Luo, J.; Deng, X.; Zhang, H.; Xu, J. Characterization and Metabolic Diversity of Flavonoids in Citrus Species. *Sci. Rep.* **2017**, *7*, 10549. [\[CrossRef\]](#) [\[PubMed\]](#)
- Chen, X.; Wang, P.; Zheng, Y.; Gu, M.; Lin, X.; Wang, S.; Jin, S.; Ye, N. Comparison of Metabolome and Transcriptome of Flavonoid Biosynthesis Pathway in a Purple-Leaf Tea Germplasm Jinmingzao and a Green-Leaf Tea Germplasm Huangdan reveals Their Relationship with Genetic Mechanisms of Color Formation. *Int. J. Mol. Sci.* **2020**, *21*, 4167. [\[CrossRef\]](#) [\[PubMed\]](#)
- Zheng, C.; Ma, J.-Q.; Ma, C.-L.; Shen, S.-Y.; Liu, Y.-F.; Chen, L. Regulation of Growth and Flavonoid Formation of Tea Plants (*Camellia sinensis*) by Blue and Green Light. *J. Agric. Food Chem.* **2019**, *67*, 2408–2419. [\[CrossRef\]](#) [\[PubMed\]](#)
- Lu, S.; Wang, J.; Zhuge, Y.; Zhang, M.; Liu, C.; Jia, H.; Fang, J. Integrative Analyses of Metabolomes and Transcriptomes Provide Insights into Flavonoid Variation in Grape Berries. *J. Agric. Food Chem.* **2021**, *69*, 12354–12367. [\[CrossRef\]](#)
- Liu, J.; Hefni, M.E.; Witthöft, C.M. Characterization of Flavonoid Compounds in Common Swedish Berry Species. *Food* **2020**, *9*, 358. [\[CrossRef\]](#)
- Cui, Q.; Liu, J.-Z.; Wang, L.-T.; Kang, Y.-F.; Meng, Y.; Jiao, J.; Fu, Y.-J. Sustainable deep eutectic solvents preparation and their efficiency in extraction and enrichment of main bioactive flavonoids from sea buckthorn leaves. *J. Clean. Prod.* **2018**, *184*, 826–835. [\[CrossRef\]](#)
- Chen, C.; Zhang, H.; Xiao, W.; Yong, Z.-P.; Bai, N. High-performance liquid chromatographic fingerprint analysis for different origins of sea buckthorn berries. *J. Chromatogr. A* **2007**, *1154*, 250–259. [\[CrossRef\]](#)
- Bagdonaitė, E.; Mártonfi, P.; Repčák, M.; Labokas, J. Variation in concentrations of major bioactive compounds in *Hypericum perforatum* L. from Lithuania. *Ind. Crops Prod.* **2012**, *35*, 302–308. [\[CrossRef\]](#)
- Smelcerovic, A.; Spitel, M.; Zuehlke, S. Comparison of Methods for the Exhaustive Extraction of Hypericins, Flavonoids, and Hyperforin from *Hypericum perforatum* L. *J. Agric. Food Chem.* **2006**, *54*, 2750–2753. [\[CrossRef\]](#) [\[PubMed\]](#)
- Gou, K.-J.; Zeng, R.; Ma, Y.; Li, A.-N.; Yang, K.; Yan, H.-X.; Jin, S.-R.; Qu, Y. Traditional uses, phytochemistry, and pharmacology of *Persicaria orientalis* (L.) Spach—A review. *J. Ethnopharmacol.* **2020**, *249*, 112407. [\[CrossRef\]](#) [\[PubMed\]](#)
- Kurkina, A.V.; Ryazanova, T.K.; Kurkin, V.A. Flavonoids from the Aerial Part of *Polygonum persicaria*. *Chem. Nat. Compd.* **2013**, *49*, 845–847. [\[CrossRef\]](#)
- Sharma, A.; Shahzad, B.; Rehman, A.; Bhardwaj, R.; Landi, M.; Zheng, B. Response of Phenylpropanoid Pathway and the Role of Polyphenols in Plants under Abiotic Stress. *Molecules* **2019**, *24*, 2452. [\[CrossRef\]](#)



15. Sathishkumar, P.; Gu, F.L.; Zhan, Q.; Palvannan, T.; MohdYusoff, A.R. Flavonoids mediated 'Green' nanomaterials: A novel nanomedicine system to treat various diseases—Current trends and future perspective. *Mater. Lett.* **2018**, *210*, 26–30. [\[CrossRef\]](#)
16. Yoon, K.D.; Lee, J.Y.; Kim, T.Y.; Kang, H.; Ha, K.S.; Ham, T.H.; Ryu, S.N.; Kang, M.Y.; Kim, Y.H.; Kwon, Y.I. In Vitro and in Vivo Anti-Hyperglycemic Activities of Taxifolin and Its Derivatives Isolated from Pigmented Rice (*Oryzae sativa* L. cv. Superhongmi). *J. Agric. Food Chem.* **2020**, *68*, 742–750. [\[CrossRef\]](#)
17. Kim, J.W.; Im, S.; Jeong, H.R.; Jung, Y.S.; Lee, I.; Kim, K.J.; Park, S.K.; Kim, D.O. Neuroprotective effects of Korean red pine (*Pinus densiflora*) bark extract and its phenolics. *J. Microbiol. Biotechnol.* **2018**, *28*, 679–687. [\[CrossRef\]](#)
18. Xia, Y.; Wang, Y.; Li, W.; Ma, C.; Liu, S. Homogenization-assisted cavitation hybrid rotation extraction and macroporous resin enrichment of dihydroquercetin from *Larixgmelinii*. *J. Chromatogr. B* **2017**, *1070*, 62–69. [\[CrossRef\]](#)
19. Ilyasov, I.R.; Beloborodov, V.L.; Selivanova, I.A. Three ABTS•+ radical cation-based approaches for the evaluation of antioxidant activity: Fast- and slow-reacting antioxidant behavior. *Chem. Paper* **2018**, *72*, 1917–1925. [\[CrossRef\]](#)
20. Ilyasov, I.; Beloborodov, V.; Antonov, D.; Dubrovskaya, A.; Terekhov, R.; Zhevlakova, A.; Saydasheva, A.; Evteev, V.; Selivanova, I. Flavonoids with Glutathione Antioxidant Synergy: Influence of Free Radicals Inflow. *Antioxidants* **2020**, *9*, 695. [\[CrossRef\]](#)
21. Schauss, A.G.; Tselyico, S.S.; Kuznetsova, V.A.; Yegorova, I. Toxicological and genotoxicity assessment of a dihydroquercetin-rich Dahurian larch tree (*Larix gmelinii* Rupr) extract (Lavitol). *Int. J. Toxicol.* **2015**, *34*, 162–181. [\[CrossRef\]](#) [\[PubMed\]](#)
22. Taldaev, A.; Terekhov, R.; Nikitin, I.; Zhevlakova, A.; Selivanova, I. Insights into the Pharmacological Effects of Flavonoids: The Systematic Review of Computer Modeling. *Int. J. Mol. Sci.* **2022**, *23*, 6023. [\[CrossRef\]](#) [\[PubMed\]](#)
23. Fischer, A.; Sellner, M.; Naranjan, S.; Smieško, M.; Lill, M.A. Potential Inhibitors for Novel Coronavirus Protease Identified by Virtual Screening of 606 Million Compounds. *Int. J. Mol. Sci.* **2020**, *21*, 3626. [\[CrossRef\]](#) [\[PubMed\]](#)
24. Raj, U.; Varadwaj, P.K. Flavonoids as multi-target inhibitors for proteins associated with Ebola virus: In-silico discovery using virtual screening and molecular docking studies. *Interdiscip. Sci.* **2016**, *8*, 132–141. [\[CrossRef\]](#)
25. Oi, N.; Chen, H.; Kim, M.O.; Kim, M.O.; Lubert, R.A.; Bode, A.M.; Dong, Z. Taxifolin Suppresses UV-Induced Skin Carcinogenesis by Targeting EGFR and PI3K. *Cancer Prev. Res.* **2012**, *5*, 1103–1114. [\[CrossRef\]](#)
26. Dias, J.L.; Lenza, M.; Ferreira, R.S. Cocrystallization: A tool to modulate physicochemical and biological properties of food-relevant polyphenols. *Trends Food Sci. Technol.* **2021**, *110*, 13–27. [\[CrossRef\]](#)
27. Selivanova, I.A.; Terekhov, R.P. Crystal engineering as a scientific basis for modification of physicochemical properties of bioflavonoids. *Russ. Chem. Bull.* **2019**, *68*, 2155–2162. [\[CrossRef\]](#)
28. Li, W.; Pi, J.; Zhang, Y.; Ma, X.; Zhang, B.; Wang, S.; Qi, D.; Li, N.; Guo, P.; Liu, Z. A strategy to improve the oral availability of baicalein: The baicalein-theophylline cocrystal. *Fitoterapia* **2018**, *129*, 85–93. [\[CrossRef\]](#)
29. Terekhov, R.; Selivanova, I. Fractal Aggregation of Dihydroquercetin After Lyophilization. *J. Pharm. Innov.* **2018**, *13*, 313–320. [\[CrossRef\]](#)
30. Liu, H.; Lin, H.; Zhou, Z.; Li, L. Bergenin-isonicotinamide (1:1) cocrystal with enhanced solubility and investigation of its solubility behaviour. *J. Drug Deliv. Sci. Tech.* **2021**, *64*, 102556. [\[CrossRef\]](#)
31. Terekhov, R.P.; Selivanova, I.A.; Tyukavkina, N.A.; Shlyov, G.V.; Utenishev, A.N.; Porozov, Y.B. Taxifolin tubes: Crystal engineering and characteristics. *Acta Crystallogr. B* **2019**, *75*, 175–182. [\[CrossRef\]](#) [\[PubMed\]](#)
32. Patil, S.; Chaudhari, K.; Kamble, R. Electrospray technique for cocrystallization of phytochemicals. *J. King Saud. Univ. Sci.* **2018**, *30*, 138–141. [\[CrossRef\]](#)
33. An, H.; Lee, Y.; Liu, L.; Lee, S.; Lee, J.; Yi, Y. Physical and Chemical Stability of Formulations Loaded with Taxifolin Tetra-octanoate. *Chem. Pharm. Bull.* **2019**, *67*, 985–991. [\[CrossRef\]](#)
34. Zu, Y.; Wu, W.; Zhao, X.; Li, Y.; Wang, W.; Zhong, C.; Zhang, Y. The high water solubility of inclusion complex of taxifolin- $\gamma$ -CD prepared and characterized by the emulsion solvent evaporation and the freeze drying combination method. *Int. J. Pharm.* **2014**, *477*, 148–158. [\[CrossRef\]](#)
35. Shikov, A.N.; Pozharitskaya, O.N.; Miroshnyk, I.; Mirza, S.; Hirsjärvi, S.; Makarov, V.G.; Heinämäki, J.; Yliruusi, J.; Hiltunen, R. Nanodispersions of taxifolin: Impact of solid-state properties on dissolution behavior. *Int. J. Pharm.* **2009**, *377*, 148–152. [\[CrossRef\]](#) [\[PubMed\]](#)
36. Hasabi, F.; Nasipour, A.; Varshosaz, J.; Gacia-Manrique, P.; Blanco-López, M.C.; Gutiérrez, G.; Matos, M. Formulation and Characterization of Taxifolin-Loaded Lipid Nanovesicles (Liposomes, Niosomes, and Transfersomes) for Beverage Fortification. *Eur. J. Lipid Sci. Technol.* **2020**, *122*, 1900105. [\[CrossRef\]](#)
37. Shubina, V.S.; Shatalin, Y.V. Skin Regeneration after Chemical Burn under the Effect of Taxifolin-Based Preparations. *Bull. Exp. Biol. Med.* **2012**, *154*, 152–157. [\[CrossRef\]](#)
38. Guo, Y.; Wang, C.; Dun, J.; Du, L.; Hawley, M.; Sun, C.C. Mechanism for the Reduced Dissolution of Ritonavir Tablets by Sodium Lauryl Sulfate. *J. Pharm. Sci.* **2019**, *108*, 516–524. [\[CrossRef\]](#)
39. Sayatan, C.; Chadan, B.; Zheng, J.; Sun, C.C. Effect of Heating Rate and Kinetic Model Selection on Activation Energy of Nonisothermal Crystallization of Amorphous Felodipine. *J. Pharm. Sci.* **2014**, *103*, 3950–3957. [\[CrossRef\]](#)
40. Poozesh, S.; Bilgili, E. Scale-up of pharmaceutical spray drying using scale-up rules: A review. *Int. J. Pharm.* **2019**, *562*, 271–292. [\[CrossRef\]](#)
41. Ziaee, A.; Albadarin, A.B.; Padrela, L.; Femmer, T.; O'Reilly, E.; Walker, G. Spray drying of pharmaceuticals and biopharmaceuticals: Critical parameters and experimental process optimization approaches. *Eur. J. Pharm. Sci.* **2019**, *127*, 300–318. [\[CrossRef\]](#) [\[PubMed\]](#)

42. Celik, M.; Wendell, S.C. Spray Drying and Pharmaceutical Applications. In *Handbook of Pharmaceutical Granulation Technology*; Parikh, D.M., Ed.; CRC Press: Boca Raton, FL, USA, 2016.
43. Singh, A.; den Mooter, G.V. Spray drying formulation of amorphous solid dispersions. *Adv. Drug Deliv. Rev.* **2015**, *100*, 27–50. [[CrossRef](#)] [[PubMed](#)]
44. Miao, X.; Zhou, J.; Liao, Y.; Zheng, Y. Chinese Medicine in Inhalation Therapy: A Review of Clinical Application and Formulation Development. *Curr. Pharm. Des.* **2015**, *21*, 3917–3931. [[CrossRef](#)] [[PubMed](#)]
45. Gharsallaoui, A.; Roudaut, G.; Chambin, O.; Voille, A.; Saurel, R. Applications of spray-drying in microencapsulation of food ingredients: An overview. *Food Res. Int.* **2007**, *40*, 1107–1121. [[CrossRef](#)]
46. Zhao, Y.; Chang, Y.-X.; Hu, X.; Liu, C.-Y.; Quan, L.-H.; Liao, Y.-H. Solid lipid nanoparticles for sustained pulmonary delivery of Yuxingcao essential oil: Preparation, characterization and in vivo evaluation. *Int. J. Pharm.* **2017**, *516*, 364–371. [[CrossRef](#)]
47. Vehring, R. Pharmaceutical Particle Engineering via Spray Drying. *Pharm. Res.* **2008**, *25*, 999–1022. [[CrossRef](#)]
48. Lauro, M.R.; Maggi, L.; Conte, U.; De Simone, F.; Aquino, R.P. Rutin and quercetin gastro-resistant microparticles obtained by spray-drying technique. *J. Drug Deliv. Sci. Technol.* **2005**, *15*, 363–369. [[CrossRef](#)]
49. Sansone, F.; Rossi, A.; Del Gaudio, P.; De Simone, F.; Aquino, R.P.; Lauro, M.R. Hesperidin Gastroresistant Microparticles by Spray-Drying: Preparation, Characterization, and Dissolution Profiles. *AAPS PharmSciTech* **2009**, *10*, 391–401. [[CrossRef](#)]
50. Sansone, F.; Picerno, P.; Mencherini, T.; Villecco, F.; D’Ursi, A.M.D.; Aquino, R.P.; Lauro, M.R. Flavonoid microparticles by spray-drying: Influence of enhancers of the dissolution rate on properties and stability. *J. Food Eng.* **2011**, *103*, 188–196. [[CrossRef](#)]
51. Lauro, M.R.; De Simone, F.; Sansone, F.; Iannelli, P.; Aquino, R.P. Preparations and release characteristics of naringin and naringenin gastro-resistant microparticles by spray-drying. *J. Drug Deliv. Sci. Technol.* **2007**, *17*, 119–124. [[CrossRef](#)]
52. Terekhov, R.P.; Selivanova, I.A.; Tyukavkina, N.A.; Ilyasov, I.R.; Zhevlakova, A.K.; Dzuban, A.V.; Bogdanov, A.G.; Davidovich, G.N.; Shylov, G.V.; Utenishev, A.N.; et al. Assembling the Puzzle of Taxifolin Polymorphism. *Molecules* **2020**, *25*, 5437. [[CrossRef](#)] [[PubMed](#)]
53. Terekhov, R.P.; Selivanova, I.A.; Anurova, M.N.; Zhevlakova, A.K.; Nikitin, I.D.; Cong, Z.; Ma, S.; Yang, F.; Dong, Z.; Liao, Y. Comparative Study of Wound-Healing Activity of Dihydroquercetin Pseudopolymorphic Modifications. *Bull. Exp. Biol. Med.* **2021**, *170*, 444–447. [[CrossRef](#)] [[PubMed](#)]
54. Mizina, P.G.; Gulenkov, A.S. The orally disintegrating tablets: The achievements and prospects (review). *Probl. Bio. Med. Pharm. Chem.* **2018**, *21*, 3–11. (In Russian) [[CrossRef](#)]
55. Ku, M.S. Use of the biopharmaceutical classification system in early drug development. *AAPS J.* **2008**, *10*, 208–212. [[CrossRef](#)]
56. Zuikina, Y.; Polovko, N.; Strilets, O.; Strelnikov, L. The in vitro release testing and the antimicrobial activity of semi-solid dosage forms which contain salicylic acid. *Farmacia* **2021**, *69*, 1073–1079. [[CrossRef](#)]
57. Thomson, K.S.; Thomson, G.K.; Biehle, J.; Deeb, A.; Crawford, J.; Herrera, R. A novel Topical Combination Ointment with Antimicrobial Activity against Methicillin-Resistant *Streptococcus aureus*, Gram-Negative Superbugs, Yeasts, and Dermatophytic Fungi. *Curr. Ther. Res. Clin. Exp.* **2016**, *83*, 8–12. [[CrossRef](#)]
58. *European Pharmacopoeia*, 10th ed.; European Directorate for the Quality of Medicines & HealthCare: Strasbourg, France, 2019.
59. Petrie, A.; Sabin, C. *Medical Statistics at a Glance*, 3rd ed.; John Wiley & Sons: New York, NY, USA, 2009.
60. MacFarland, T.W.; Yates, J.M. Mann-Whitney U Test. In *Introduction to Nonparametric Statistics for the Biological Science Using R*; Springer International Publishing AG: Cham, Switzerland, 2016; pp. 103–132.
61. Shkarenkov, A.A.; Beloshapko, A.A.; Kuznetsov, Y.B.; Borovkova, M.V.; Anikanova, V.V.; Krepkova, L.V. Preclinical toxicological study of Diquertin. *Probl. Biol. Med. Pharm. Chem.* **1998**, *3*, 36–39. (In Russian)
62. Kolkhir, V.K.; Tyukavkina, N.A.; Bykov, V.A.; Glyzin, V.I.; Arzamastsev, A.P.; Baginskaya, A.I.; Sokolov, S.Y.; Kolesnik, Y.A.; Glazova, N.G.; Rulenko, I.A.; et al. Dicvertin: A New Antioxidant and Capillary-Protecting Drugs. *Pharm. Chem. J.* **1995**, *29*, 657–660. [[CrossRef](#)]
63. Kolkhir, V.K.; Bykov, V.A.; Teselkin, Y.O.; Babenkova, I.V.; Tyukavkina, N.A.; Rulenko, I.A.; Kolesnik, Y.A.; Eichholz, A.A. Use of a new antioxidant diquertin as an adjuvant in the therapy of patients with acute pneumonia. *Phytother. Res.* **1998**, *12*, 606–608. [[CrossRef](#)]
64. Fang, Y.; Cao, W.; Xia, M.; Pan, S.; Xu, X. Study of structure and permeability relationship of flavonoids in caco-2 cells. *Nutrients* **2017**, *9*, 1301. [[CrossRef](#)]
65. Wong, M.; McAllister, M. Lead Identification/Optimization. In *Oral Formulation Roadmap from Early Drug Discovery to Development*; Kwong, E., Ed.; John Wiley & Sons Inc: Hoboken, NJ, USA, 2017; pp. 9–38.
66. Liu, W.; Okochi, H.; Benet, L.Z.; Zhai, S.-D. Sotalol permeability in cultured-cell, rat intestine and PAMPA system. *Pharm. Res.* **2012**, *29*, 1768–1774. [[CrossRef](#)] [[PubMed](#)]
67. Zu, Y.; Wu, W.; Zhao, X.; Li, Y.; Wang, W.; Zhong, C.; Zhang, Y.; Zhao, X. Enhancement of solubility, antioxidant ability and bioavailability of taxifolin nanoparticles by liquid antisolvent precipitation technique. *Int. J. Pharm.* **2014**, *471*, 366–376. [[CrossRef](#)]
68. Zu, S.; Yang, L.; Huang, J.; Ma, C.; Wang, W.; Zhao, C.; Zu, Y. Micronization of Taxifolin by Supercritical Antisolvent Process and Evaluation of Radical Scavenging Activity. *Int. J. Mol. Sci.* **2012**, *13*, 8869–8881. [[CrossRef](#)] [[PubMed](#)]
69. Potoroko, I.Y.; Kalinina, I.V.; Naumenko, N.V.; Fatkullin, R.I.; Nenashcheva, A.V.; Uskova, D.G.; Sonawane, S.H.; Ivanova, D.G.; Velyamov, M.T. Sonochemical micronization of taxifolin aimed at improving its bioavailability in drinks for athletes. *Hum. Sport Med.* **2018**, *18*, 90–100. [[CrossRef](#)]

70. Bavishi, D.D.; Borkhataria, C.H. Spring and parachute: How cocrystals enhance solubility. *Prog. Cryst. Growth Charact. Mater.* **2016**, *62*, 1–8. [[CrossRef](#)]
71. Smith, A.J.; Kavuru, P.; Arora, K.K.; Kesani, S.; Tan, J.; Zaworotko, M.J.; Shytle, R.D. Crystal engineering of green tea epigallocatechin-3-gallate (EGCg) cocrystals and pharmacokinetic modulation in rats. *Mol. Pharm.* **2013**, *10*, 2948–2961. [[CrossRef](#)]
72. Wang, C.; Tong, Q.; Hou, X.; Hu, S.; Fang, J.; Sun, C.C. Enhancing Bioavailability of Dihydromyricetin through Inhibiting Precipitation of Soluble Cocrystals by a Crystallization Inhibitor. *Cryst. Growth Des.* **2016**, *16*, 5030–5039. [[CrossRef](#)]
73. Kassem, F.A.; Abdelaziz, A.E.; El Maghraby, G.M. Ethanol-assisted kneading of apigenin with arginine for enhanced dissolution rate of apigenin: Development of rapidly disintegrating tablets. *Pharm. Dev. Tech.* **2021**, *26*, 693–700. [[CrossRef](#)]
74. Shevelev, A.B.; la Porta, N.; Isakova, E.P.; Martens, S.; Biryukova, Y.K.; Belous, A.S.; Sivokhin, D.A.; Trubnikova, E.V.; Zylkova, M.V.; Belyakova, A.V.; et al. In Vivo Antimicrobial and Wound-Healing Activity of Resveratrol, Dihydroquercetin, and Dihydromyricetin against *Staphylococcus aureus*, *Pseudomonas aeruginosa*, and *Candida albicans*. *Pathogens* **2020**, *9*, 296. [[CrossRef](#)]
75. Ivanov, M.; Novović, K.; Malešević, M.; Dinić, M.; Stojković, D.; Jovčić, B.; Soković, M. Polyphenols as Inhibitors of Antibiotic Resistant Bacteria-Mechanisms Underlying Rutin Interference with Bacterial Virulence. *Pharmaceuticals* **2022**, *15*, 385. [[CrossRef](#)]
76. Abugri, D.A.; Witola, W.H.; Russel, A.E.; Troy, R.M. In vitro activity of the interaction between taxifolin (dihydroquercetin) and pyrimethamine against *Toxoplasma gondii*. *Chem. Biol. Drug Des.* **2018**, *91*, 194–201. [[CrossRef](#)]
77. Taldaev, A.K.; Terekhov, R.P.; Selivanova, I.A. Antimicrobial activity of dihydroquercetin against *E. coli*. In *Mendeleev 2021. Book of Abstracts XII International Conference on Chemistry for Young Scientists*; VVM Publishing LLC: Saint-Petersburg, Russia, 2021; p. 172.
78. Terekhov, R.P.; Selivanova, I.A. Molecular modeling of the interaction of the dihydroquercetin and its metabolites with cyclooxygenase-2. *Bull. Sib. Med.* **2019**, *18*, 101–106. (In Russian) [[CrossRef](#)]
79. Ha, C.H.H.; Fatima, A.; Gaurav, A. In silico investigation of flavonoids as potential trypanosomal nucleoside hydrolase inhibitors. *Adv. Bioinforma* **2015**, *12*, 1–10. [[CrossRef](#)] [[PubMed](#)]
80. Abdulrazzak, S.A.; Vorobyev, A.N.; Sinitsyna, N.I.; Sharutina, I.V.; Menshova, O.V.; Elizarova, E.V.; Ivanova, Y.V.; Karamyan, A.S.; Abramovich, R.A.; Potanina, O.G.; et al. Development of Dihydroquercetin-based Oral tablets and Evaluation of the General Toxic Effect. *Drug Dev. Regist.* **2022**, *11*, 126–138. (In Russian) [[CrossRef](#)]
81. Peltonen, L.; Strachan, C.J. Degrees of order: A comparison of nanocrystal and amorphous solids for poorly soluble drugs. *Int. J. Pharm.* **2020**, *586*, 119492. [[CrossRef](#)]
82. Murdande, S.B.; Pikal, M.J.; Shanker, R.M.; Bogner, R.H. Solubility advantage of amorphous pharmaceuticals: I. A thermodynamic analysis. *J. Pharm. Sci.* **2010**, *99*, 1254–1264. [[CrossRef](#)]